Residual Velocities in Steady Free Boundary Value Problems of Vector Laplacian Type

Wan Chen * Brian Wetton †

February 1, 2008

Abstract

This paper describes a technique to determine the linear well-posedness of a general class of vector elliptic problems that include a steady interface, to be determined as part of the problem, that separates two subdomains. The interface satisfies mixed Dirichlet and Neumann conditions. We consider "2+2" models, meaning two independent variables respectively on each subdomain. The governing equations are taken to be vector Laplacian, to be able to make analytic progress. The interface conditions can be classified into four large categories, and we concentrate on the one with most physical interest. The well-posedness criteria in this case are particularly clear. In many physical cases, the movement of the interface in time-dependent situations can be reduced to a normal motion proportional to the residual in one of the steady state interface conditions (the elliptic interior problems and the other interface conditions are satisfied at each time). If only the steady state is of interest, one can consider using other residuals for the normal velocity. Our analysis can be extended to give insight into choosing residual velocities that have superior numerical properties. Hence, in the second part, we discuss an iterative method to solve free boundary problems. The advantages of the correctly chosen, non-physical residual velocities are demonstrated in a numerical example, based on a simplified model of two-phase flow with phase change in porous media.

*Department of Mathematics, UBC, wanchen@math.ubc.ca

†corresponding author, Department of Mathematics, UBC, wetton@math.ubc.ca.

Keywords: Well-Posedness, Free Boundary Problem, Residual Velocity.

1 Introduction

Free boundary problems (FBPs) have motivated several studies in the past due to their vast applications in fluid flow, phase change models and other fields. Some classical free boundary problems are: the dam seepage problem [6], incompressible two-phase flow [5, 14] (*i.e.* falling droplets or rising bubbles [12], the Alt-Caffarelli problem [2], the classical Stefan problem [6], etc. From a mathematical point of view, FBPs are boundary value problems with an unknown boundary. The motion (unsteady case) or position (steady case) of the boundary has to be determined together with the solution of the given partial differential equations on one (free surface) or both sides (interface) of the free boundary. The coupling of the free boundary to the interior is always nonlinear [13], and thus FBPs are often not easy to solve.

The common structure of all the examples above is that at steady state, they all have second order elliptic governing equations for m unknowns on one side and n unknowns on the other side of the free boundary. We denote this situation as an "m+n" problem. There must then be $m+n+1$ Dirichlet-Neumann conditions at the interface. For fourth order problems such as biharmonic equation, we would need $2m + 2n + 1$ conditions at the interface to determine an "m+n" problem. By this generalization, many more complicated problems can be formulated. However, fourth order problems and second order elliptic systems other than vector Laplacian are not considered further in this present study.

To solve free boundary problems numerically there are three main kinds of methods: capturing methods, front tracking methods and level set methods. Capturing methods are based on Eulerian formulation and the problems are reformulated and solved in the whole domain. The interface location is recovered from the discrete solution. In these methods, the interface conditions are not specified explicitly. A classical example is the Enthalpy method [6]. The alternative is to discretize the interface explicitly [16] [18] or via a level set approach [11]. In both these cases, the interface conditions (and interface velocity for time-dependent problems) are implemented explicitly. This can be done by considering the domains as disjoint and discretizing

the equations and interface conditions directly [8] or by discretizing the entire domain and modifying the discretization near the interface [10]. The latter approach combined with modern level set techniques can also be considered a capturing method.

In a few cases, steady state solutions can be obtained directly using shape optimization [13, 9]. Another approach to reach steady state solutions is to solve the transient time-dependent problem to long time. In the class of problems we consider, the normal motion of the interface is driven by the difference of solutions on either side of the interface. For example, solidification boundaries are driven by a Stefan condition [6]. It should be made clear that we are not considering here the problem of dendritic growth [1, 4] which in our framework would be ill-posed, but is regularized by higher order (curvature) terms. We consider only well-posed problems which do not need regularization. In the physical example of section 3, the interface is moved by the net mass flux at the interface. Those are typical conditions that give normal velocity of each point on the interface. In these examples and others of physical interest, the normal interface velocity is given by the residual in one of the steady state interface conditions. In this paper, we apply the residual velocity method (a tracking technique) of [7]:

1. Given an initial interface Γ and tracking points $\{\mathbf{x} : \mathbf{x} \in \Gamma\}$, solve numerically a fixed boundary value problem satisfying all of the steady interface conditions but one.
2. Substitute the solutions into the unsatisfied condition and find the residual $R(\mathbf{x})$.
3. If the residual is larger than a tolerance, explicitly evolve the interface using the residual as a normal velocity of the tracking points:
$$\mathbf{V}_n = R(\mathbf{x})$$
4. Repeat the process until the residual is less than a given tolerance.

At termination, all interface conditions are approximately satisfied. This is an example of a *value* method [15] (since it uses only values of the solution not shape derivatives to update the interface). In this algorithm, the choice of residual velocity is not specified, so we can choose different interface conditions and their combinations as the residual velocity, not only the real, physical velocity. As a result, we

can show both analytically and numerically that the residual velocity chosen by our criteria has better numerical properties than the physical one. Specifically, our method can use time steps independent of mesh size in the explicit step 3 above. Because of the use of an artificial interface velocity, our method provides accurate solutions only at steady state.

There are few publications addressing the analytic theory of the general class of the steady free boundary problems considered here. In [7] the authors present a linear theory of the well-posedness of the general class of "1+1" Laplacian problems. Our work is an extension of [7]. Specifically, the ideas considered there for the scalar case are extended to the "2+2" case. An analytic simplification to the well-posedness is identified in a physically important class of problems. The class is represented by a simplified model of two-phase flow with phase change in porous media. In addition, a different numerical implementation of the corresponding residual velocity method is given. While the numerical method is not as general as that of [7] it does show that accurate results can be obtained without grid refinement at the interface. Attaining this in more general codes is a goal for future work.

The framework of this paper is following: In section 2, we discuss the four classes of second order "2+2" problems with different combinations of Dirichlet-Neumann conditions. A physically interesting example, a simplified model of two-phase flow with phase change in porous media, is presented in section 3. In section 4, well-posedness criteria of "2+2" Laplacian equations from [7] are reviewed and applied to the example and generalized. The extension to 3-D problem has been shown as well. Then in section 5, the example of vector Laplacian type free boundary problem are computed numerically, using a finite difference method in mapped coordinates (a so-called fictitious domain method [9]). The performances of both physical velocity and our residual velocity are compared, and the results agree with the analytical predictions.

2 Class Division of "2+2" Problems

Consider a two-dimensional model, when $m = n = 2$. We have a "2+2" vector elliptic problems for variables $u^{\pm}, p^{\pm}$, assuming that $\mathbf{L_1}(u^+, p^+) = 0$ in the upper subdomain D^+ and $\mathbf{L_2}(u^-, p^-) = 0$ in

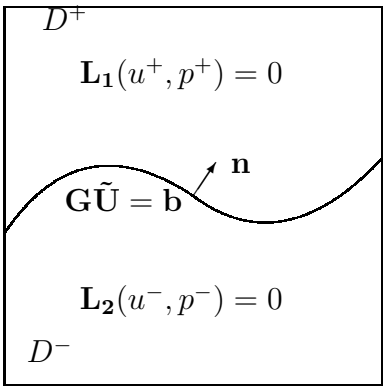

Figure 1: The model of second order "2+2" problems. $\mathbf{L_{1,2}}$ are linear, second order elliptic operators and there are five interface conditions represented by $\mathbf{G}$.

the lower subdomain D^-, as shown in Fig. 1. There are five conditions at the interface. Here, we consider $\mathbf{L_1}$ and $\mathbf{L_2}$ to be general, vector, linear, second order elliptic operator but in our analysis below we consider only the case of $\mathbf{L_{1,2}}$ both being the vector Laplacian.

The five Dirichlet-Neumann boundary conditions at Γ in matrix form, will be:

$$\mathbf{G\tilde{U}} \;=\; \mathbf{b}. \tag{1}$$

where $\mathbf{G}$ is a 5×8 matrix, and $\mathbf{\tilde{U}^T} = (u^+_{\mathbf{n}},\ u^-_{\mathbf{n}},\ p^+_{\mathbf{n}},\ p^-_{\mathbf{n}},\ u^+,\ u^-,\ p^+,\ p^-)$ is a vector composed of all unknown variables and their normal ($\mathbf{n}$ pointing from D^- to D^+) derivatives at the interface. The matrix $\mathbf{G}$ can be split naturally into two parts:

$$\mathbf{G} = (G_N \;\mid\; G_D)$$

where G_N and G_D are 5×4 sub-matrices, representing respectively Neumann conditions and Dirichlet conditions.

We use the rank r of G_N (or equivalently the number $5-r$ of pure Dirichlet conditions) as the criteria to classify possible forms of $\mathbf{G}$. As a result, there are four classes of boundary conditions corresponding to r=4, 3, 2, 1 below. Normal forms can be obtained using the following allowable operations:

1. Row operations on $\mathbf{G}$.
2. Simultaneous swap of columns 1 and 2, 3 and 4, 5 and 6, 7 and 8. This swap is accompanied by a sign change of columns 1-4. (corresponds to a relabelling of D^- and D^+).
3. Column operations between columns 1 and 3 with identical operations on columns 5 and 7 (linear combination of unknowns in

D^+).

4. Column operations between columns 2 and 4 with identical operations on columns 6 and 8 (linear combination of unknowns in D^-).

The following generic forms result:

Class A: One pure Dirichlet condition, and thus the rank of G_N is 4:

$$\mathbf{G} = \left(\begin{array}{cccc|cccc} 1 & 0 & 0 & 0 & 0 & G_{1,6} & G_{1,7} & G_{1,8} \\ 0 & 1 & 0 & 0 & 0 & G_{2,6} & G_{2,7} & G_{2,8} \\ 0 & 0 & 1 & 0 & 0 & \cdots & \cdots & \cdots \\ 0 & 0 & 0 & 1 & 0 & \cdots & \cdots & \cdots \\ 0 & 0 & 0 & 0 & 1 & 0 & G_{5,7} & G_{5,8} \end{array}\right)$$

Class B: Two pure Dirichlet conditions, and the rank of G_N is 3.

$$\mathbf{G} = \left(\begin{array}{cccc|cccc} 1 & 0 & 0 & G_{1,4} & 0 & 0 & G_{1,7} & G_{1,8} \\ 0 & 1 & 0 & G_{2,4} & 0 & 0 & G_{2,7} & G_{2,8} \\ 0 & 0 & 1 & G_{3,4} & 0 & 0 & G_{3,7} & G_{3,8} \\ 0 & 0 & 0 & 0 & G_{4,5} & G_{4,6} & G_{4,7} & G_{4,8} \\ 0 & 0 & 0 & 0 & G_{5,5} & G_{5,6} & G_{5,7} & G_{5,8} \end{array}\right)$$

where the last two rows are linearly independent but no further reduction is possible.

Class C: Three pure Dirichlet conditions:

$$\mathbf{G} = \left(\begin{array}{cccc|cccc} G_{1,1} & G_{1,2} & G_{1,3} & G_{1,4} & 0 & 0 & 0 & G_{1,8} \\ G_{2,1} & G_{2,2} & G_{2,3} & G_{2,4} & 0 & 0 & 0 & G_{2,8} \\ 0 & 0 & 0 & 0 & 1 & 0 & 0 & G_{3,8} \\ 0 & 0 & 0 & 0 & 0 & 1 & 0 & G_{4,8} \\ 0 & 0 & 0 & 0 & 0 & 0 & 1 & G_{5,8} \end{array}\right)$$

where the first two row vectors restricted to the left block are linearly independent but no further reduction is possible.

Class D: Four pure Dirichlet conditions:

$$\mathbf{G} = \left(\begin{array}{cccc|cccc} 1 & 0 & G_{1,3} & G_{1,4} & 0 & 0 & 0 & 0 \\ 0 & 0 & 0 & 0 & 1 & 0 & 0 & 0 \\ 0 & 0 & 0 & 0 & 0 & 1 & 0 & 0 \\ 0 & 0 & 0 & 0 & 0 & 0 & 1 & 0 \\ 0 & 0 & 0 & 0 & 0 & 0 & 0 & 1 \end{array}\right)$$

Class C is arguably of most physical interest. If the vector elliptic equations represent conservation of two quantities with fluxes proportional to gradients, then the conservation of these quantities at the interface are represented by exactly two pure ($G_{1,8}$ and $G_{2,8}$ both zero) Neumann conditions. We define the subclass $\tilde{C}$ to be the one with these additional conditions. In the following section, we present a physical example in this class originally derived from [3]. Class D always leads to a single pure Neumann condition. We define subclasses $\tilde{A}$ and $\tilde{B}$ to be the ones with four and three, respectively, pure Neumann conditions.

3 Physical example

We consider now a physical problem involving two-phase flow with phase change in porous media. Consider a closed system consisting of a sand pack, water vapour and liquid water. If the system is heated at the top, vapour is formed, and in some cases, two distinct zones with free boundary will be observed. In the upper zone D^+, there is only vapour, while in the lower zone D^-, two-phase vapour and liquid water can be found. This model is studied in [3].

In the upper region D^+, the variable $P_v(x,t)$ and temperature $T^+(x,t)$ describe the vapour region, and the governing equations are:

$$\Delta T^+ = 0 \tag{2}$$

$$\nabla \cdot (\rho_v \mathbf{u}_v) = 0 \tag{3}$$

where ρ_v and $\mathbf{u}_v$ denote density and velocity of the vapour respectively, which are the functions of temperature T^+ and pressure P_v. According to Darcy's law, we have:

$$\mathbf{u}_v = -\frac{\kappa}{\mu_v}\nabla P_v$$

with κ the permeability and μ_v the dynamic viscosity. If we assume the gas is ideal, then:

$$\rho_v = \frac{M}{R}\frac{P_v}{T^+}$$

where M is molar mass of water, R is the universal gas constant. So the equation (3) becomes:

$$\nabla \cdot (\frac{P_v}{T^+}\nabla P_v) = 0 \tag{4}$$

Then (2) and (4) give an elliptic problem for P_v and T^+.

Flow in the lower two-phase region is described by temperature T^- and saturation $s(x, y)$. The saturation is the fraction of pore space occupied by liquid water. Energy conservation and mass conservation give us:

$$\nabla \cdot (K \nabla T^-) - h_{vap} \nabla \cdot (\rho_v \mathbf{u}_v) = 0 \quad (5)$$

$$\nabla \cdot (\rho_l \mathbf{u}_l + \rho_v \mathbf{u}_v) = 0 \quad (6)$$

where $\mathbf{u}_l, \mathbf{u}_v$ and ρ_v are functions of T^- and s. Darcy's law includes the relative permeabilities as well as the capillary pressure, which we assume are functions of the s:

$$\mathbf{u}_v = -\frac{\kappa}{\mu_v}(1-s)^3 \nabla P_{sat}(T^-)$$

$$\mathbf{u}_l = -\frac{\kappa}{\mu_l} s^3 \nabla (P_{sat}(T^-) - P_c(s))$$

where μ_v, μ_l are respectively dynamical viscosities of the vapour and liquid, P_{sat} is the saturation vapour pressure, and $P_c = P_v - P_l$ is the capillary pressure. Since evaporation and condensation rates scale to be very large in a porous media, we assume $P_v = P_{sat}(T^-)$. Therefore in the two-phase region, we have an elliptic problem for T^- and s.

On the free boundary, There are five Dirichlet-Neumann conditions required for the problem of four variables:

$s = 0$	saturation is zero at the interface
$[T] = 0$	temperature is continuous
$[P_v] = 0$	vapour pressure is continuous
$(\rho_v \mathbf{u}_v)^+ \cdot \mathbf{n} = (\rho_v \mathbf{u}_v + \rho_l \mathbf{u}_l)^- \cdot \mathbf{n}$	mass conservation
$[K T_{\mathbf{n}}] = h_{vap}(\rho_l \mathbf{u}_l) \cdot \mathbf{n}$	heat conservation

where $[\cdot]$ denotes the difference between counterparts on each side of the interface. For example: $[T] = T^+ - T^-$.

In order to make progress on this problem in our framework, considerable simplification is needed. Specifically, we need to simplify the problem to get a vector Laplacian operator on each subdomain and linear interface conditions. The model derived below lacks several aspects of physical interest and mathematical difficulty. However, it does retain the underlying structure of two elliptic systems coupled by five mixed Dirichlet-Neumann conditions at the interface. First,

we set $P_v/T^+ = 1$ in (4), which means the vapour density doesn't change. This leads to Laplacian equation of pressure: $\Delta P = 0$, then in the upper region D^+, we have:

$$\Delta P = 0, \quad \Delta T^+ = 0$$

In the lower region D^-, we simplify using the assumption that evaporation or condensation only happens at the interface. Moreover, we assume the relative permeability of vapour and liquid in D^- is independent of saturation s, the capillary pressure P_c is linear in s and saturation vapour pressure P_{sat} is linear in T^-. In the end, (5) and (6) can be reduced to two Laplacian equations:

$$\Delta s = 0, \quad \Delta T^- = 0.$$

Correspondingly, the interface conditions are given:

$$\begin{aligned}
s = 0 &\qquad \text{saturation is zero across interface} \\
[T] = 0 &\qquad \text{temperature is continuous} \\
P = T^- &\qquad \text{Vapour pressure is continuous} \\
[KT_{\mathbf{n}}] = -s_{\mathbf{n}} &\qquad \text{heat flux is continuous} \\
P_{\mathbf{n}} = T^-_{\mathbf{n}} + s_{\mathbf{n}} &\qquad \text{mass conservation}
\end{aligned}$$

Note that in the example, the interface is featured by $s = 0$, and its movement is driven by the mass flux going through the interface, so we say the physical residual velocity comes from the last Neumann condition. The five conditions can be written in matrix form (1) where $\mathbf{G}$ and $\tilde{\mathbf{U}}$ are respectively:

$$\mathbf{G} = \begin{pmatrix}
0 & 0 & 0 & 0 & 0 & 0 & 0 & 1 \\
0 & 0 & 0 & 0 & 1 & -1 & 0 & 0 \\
0 & 0 & 0 & 0 & 0 & 1 & -1 & 0 \\
K^+ & -K^- & 0 & +1 & 0 & 0 & 0 & 0 \\
0 & -1 & 1 & -1 & 0 & 0 & 0 & 0
\end{pmatrix} \tag{7}$$

and

$$\tilde{\mathbf{U}}^{\mathbf{T}} = (T^+_{\mathbf{n}},\ T^-_{\mathbf{n}},\ P_{\mathbf{n}},\ s_{\mathbf{n}},\ T^+,\ T^-,\ P,\ s)$$

Clearly, the boundary conditions are composed of three pure Dirichlet and two pure Neumann conditions, which belongs to Class $\tilde{C}$ identified in the last section.

4 Linear Well-Posedness and Residual Velocities

In the first subsection below we review briefly the theory developed in [7] targeted to the "2+2" case. Later, we identify situations where the analysis gives particularly clear insight. These include the physically important case $\tilde{C}$ identified in the previous section. Application of the theory to the example above is done, and a residual velocity with superior numerical properties is identified.

4.1 General Theory

4.1.1 Base Solutions

We find base solutions in 2D (coordinates x and y) with a flat interface $y = 0$. Take $\mathbf{u}_0^T = (u^+, u^-, p^+, p^-)$ to be the base solution of the FBP satisfying:

$$\Delta \mathbf{u}_0 = 0 \qquad \text{in } y > 0 \text{ and } y < 0 \tag{8}$$

with interface conditions:

$$\mathbf{G}\,\tilde{\mathbf{U}}_\mathbf{0} = \mathbf{b} \qquad \text{on the interface } y = 0 \tag{9}$$

where $\tilde{\mathbf{U}}_0 = \begin{pmatrix} \mathbf{u}_{0\mathbf{n}} \\ \mathbf{u}_0 \end{pmatrix}$.

We consider base solutions independent of x with $\mathbf{b}$ constant, so (8) can be reduced to $\mathbf{u}_{0yy} = 0$ and $\mathbf{u}_0$ is linearly dependent on y. That yields:

$$\mathbf{u}_0 = y\,\mathbf{r}^1 + \mathbf{r}^0$$

where

$$\tilde{\mathbf{U}}_\mathbf{0} = \begin{pmatrix} \mathbf{r}^1 \\ \mathbf{r}^0 \end{pmatrix}$$

is a constant vector solving (9). The base solution is composed of a particular solution and homogeneous solution

$$\tilde{\mathbf{U}}_\mathbf{0} = \tilde{\mathbf{r}}_H + \tilde{\mathbf{r}}_P,$$

with $\mathbf{G}\tilde{\mathbf{r}}_H = \mathbf{0}$. Hence, $\tilde{\mathbf{r}}_H$ belongs to the nullspace of $\mathbf{G}$, and $\mathcal{N}(\mathbf{G})$ has rank 3.

In order to specify a unique solution, we need three more conditions denoted by a vector $\mathbf{q} = (q_1, q_2, q_3)^T$, corresponding to the ordering of a basis of vectors of $\mathcal{N}(\mathbf{G})$, so

$$\tilde{\mathbf{U}}_0 = \begin{pmatrix} \mathbf{r}^1 \\ \mathbf{r}^0 \end{pmatrix} = \mathcal{N}(\mathbf{G}) \cdot \mathbf{q}$$

where we mean (with a slight abuse of notation) by $\mathcal{N}(\mathbf{G})$ the 8×3 matrix with a basis for this space in columns.

Consider the base solution found above to describe the local behaviour of the interface near a point, where the coordinate system has been rotated so that the local tangent plane is $y = 0$. This local base solution depends on the local data $\mathbf{b}$ and also the vector $\mathbf{q}$, which we refer to as the global fluxes. This represents the dependence of the local solution on far field conditions.

4.1.2 Linear well-posedness

We consider how small perturbation of boundary conditions about a flat interface affect the solution:

$$\mathbf{G}\tilde{\mathbf{U}} = \mathbf{b} + \epsilon \mathbf{f} e^{i\alpha x} \tag{10}$$

where $\mathbf{f}$ is a constant, α is the Fourier mode, and ϵ is a small parameter. As a result, we will obtain a new solution and new free boundary. If we can show that the linearized solution depends continuously on the data $\mathbf{f}$ for each α we say the problem is linearly well-posed.

After we perturb the interface condition using (10), we expect the new solution $\mathbf{u}$ and free boundary $y = \eta(x)$ to be in the form:

$$\begin{aligned} \mathbf{u}(x, y) &= \mathbf{u}_0(y) + \epsilon \mathbf{u}_1(x, y) + O(\epsilon^2) \\ \eta(x) &= \epsilon \eta_1(x) + O(\epsilon^2) \end{aligned}$$

where $\mathbf{u}_0, \eta_0(x)$ are the base solution from section 4.1.1 above. Following [7] it is known that linear perturbations are of the form:

$$\eta_1(x) = \tilde{\eta_1} e^{i\alpha x} \tag{11}$$

$$\mathbf{u}(x, y) = \mathbf{c} e^{\mp|\alpha| y} e^{i\alpha x} \tag{12}$$

where (12) arises from the separable solution of the Laplace operator in half planes and the sign is chosen appropriately depending on whether the corresponding variable is in the upper or lower domain,

respectively. Again following [7], if the forms (11) and (12) are put in to (10) the first order term results in the following algebraic condition:

$$\mathbf{GMc} + \hat{\eta}_1 \mathbf{G}\tilde{\mathbf{U}}_{0\mathbf{n}} = \mathbf{f} \tag{13}$$

where

$$\mathbf{M} = \begin{pmatrix} -|\alpha| & 0 & 0 & 0 \\ 0 & |\alpha| & 0 & 0 \\ 0 & 0 & -|\alpha| & 0 \\ 0 & 0 & 0 & |\alpha| \\ 1 & 0 & 0 & 0 \\ 0 & 1 & 0 & 0 \\ 0 & 0 & 1 & 0 \\ 0 & 0 & 0 & 1 \end{pmatrix}$$

and

$$\tilde{\mathbf{U}}_{0\mathbf{n}} = \begin{pmatrix} \mathbf{u}_{0yy} \\ \mathbf{u}_{0y} \end{pmatrix}$$

evaluated at $y = 0$. This can be written as:

$$\tilde{\mathbf{U}}_{0\mathbf{n}} = \mathcal{S}\tilde{\mathbf{U}}_{\mathbf{0}}$$

where $\tilde{\mathbf{U}}_{\mathbf{0}}$ is the vector from the base solution (1) and $\mathcal{S}$ is a shift matrix that moves rows 1-4 to rows 5-8 and then zeros the first four rows.

Considering (13), the well-posedness criteria can be reduced to the existence and uniqueness of $(\mathbf{c}, \hat{\eta}_1)$ for every $\mathbf{f}$ and α. Consider the matrix $\mathbf{GM}$. It is a 5×4 matrix with rank 4. We denote a vector in its left nullspace by $\mathbf{w} = \mathcal{N}[(\mathbf{GM})^T]$. Thus to ensure the well-posedness of the problem, we require:

$$\mathbf{w^T G}\tilde{\mathbf{U}}_{0\mathbf{n}} \neq 0 \tag{14}$$

This is the algebraic condition for linear well-posedness for the general class of steady free boundary value problems we have considered.

4.1.3 Residual velocity choice

In our numerical algorithm, we solve a fixed boundary problem each iteration with some of the boundary conditions in $\mathbf{G}$ satisfied, while the residual in the remaining condition is used as the normal velocity to evolve the interface. With the well-posedness criteria of the problems established above, we can discuss the stability of the numerical

methods for the free boundary problem. We consider residual velocity methods as discussed in the introduction. The only time dependence is in the interface position $y = \eta(x,t)$ which in the linearized setting above reduces to

$$y = \tilde{\eta} e^{i\alpha x} e^{\lambda t}$$

The stiffness λ is a function of the choice of residual to use as velocity and also the wave number α. If for a given residual velocity choice, $Re(\lambda) < 0$ for all α, the resulting method will converge to the steady interface solution. We show how in addition residual velocities can be chosen in some cases so that λ is bounded independently of α, which suggests that time steps for the resulting method can be chosen independently of the spatial discretization. This is verified in the example computation in the next section.

Again, following [7] the linear analysis leads to

$$\lambda = \frac{\mathbf{w^T G \tilde{U}_{0n}}}{\mathbf{w^T v}} \tag{15}$$

where $\mathbf{v}$ denotes the linear combination of residuals used as the normal velocity (the orthogonal combinations are used as interface conditions at each time) and as before $\mathbf{w^T}$ is the left nullspace of $\mathbf{GM}$.

Note that in the numerator of (15) is the well-posedness term (14). We assume we are only trying to compute solutions to well-posed problems, so can assume this term does not change sign. Thus, the stability of the scheme depends only on the denominator which depends on a straight-forward way on the velocity choice $\mathbf{v}$.

4.1.4 Discussion

The well-posedness condition (14) and stability condition (15) are powerful analytic tools. The influence of the boundary conditions (through $\mathbf{G}$), the elliptic problem (through $\mathbf{w}$ coming from $\mathbf{M}$), and boundary and far-field data (through $\mathbf{\tilde{U}_{0n}}$) are encoded in these scalar relationships. However, for problems of size "2+2" and larger, it becomes difficult to make general statements about a particular problem. In general, for "2+2" problems, $\mathbf{w}$ has elements that are fourth order polynomials in $|\alpha|$. Thus, (14) will in general also be a fourth order polynomials in $|\alpha|$, with coefficients depending on boundary data and global fluxes. We discuss below situations of physical interest (including the main example from the last section) where significant simplification occurs in these expressions.

4.2 Application to physical example

Let's go back to the concrete example in section 3 where $\mathbf{G}$ is given in (7). The nullspace of $\mathbf{G}$, $\mathcal{N}(\mathbf{G})$, is:

$$\mathcal{N}(\mathbf{G})^T = \begin{pmatrix} \frac{K^-}{K^+} & 1 & 1 & 0 & 0 & 0 & 0 & 0 \\ -\frac{1}{K^+} & 0 & +1 & +1 & 0 & 0 & 0 & 0 \\ 0 & 0 & 0 & 0 & 1 & 1 & 1 & 0 \end{pmatrix} \tag{16}$$

Each row of the matrix above corresponds to the effect of one global flux. We describe the physical interpretations of these global fluxes below:

q_1**:** This corresponds physically to a heat flux downwards in the lower region. This heat flux is balanced by a heat flux in the upper region. In addition, the temperature gradient in the lower region drives a vapour flux there that is matched by a pressure driven gradient flow in the upper region.

q_2**:** This corresponds physically to a flux of water downwards in the lower region. This flux is generated by condensation at the two phase boundary which is provided by vapour flow downwards and heat flow upwards in the upper region.

q_3**:** This term represents an additive shift in temperature and pressure.

The data term $\mathbf{b}$ is zero in this example, so the well-posedness is determined entirely by the global fluxes. Specifically, the term $\tilde{\mathbf{U}}_{\mathbf{0n}}$ in (14) and (15) is given by

$$\tilde{\mathbf{U}}_{\mathbf{0n}} \in \mathcal{S}[\mathcal{N}(\mathbf{G})] = \begin{pmatrix} 0 & 0 & 0 & 0 & \frac{K^-}{K^+} & 1 & 1 & 0 \\ 0 & 0 & 0 & 0 & -\frac{1}{K^+} & 0 & +1 & +1 \\ 0 & 0 & 0 & 0 & 0 & 0 & 0 & 0 \end{pmatrix}^T$$

where by the last term above we mean the span of the column vectors, which has rank 2. This is our first simplification: that only two of the global fluxes (the first two described above) enter the stability condition. Upon reflection, it is clear that shifting the overall temperature and pressure (the effect of q_3) in this linear problem should not affect the stability of the problem.

We now find the left nullspace $\mathbf{w}$ of $(\mathbf{GM})^T$:

$$\mathbf{w^T} = (\frac{K^+ + K^- + 2}{K^+ + K^-}|\alpha|,\ \frac{-2K^+}{K^+ + K^-}|\alpha|,\ -|\alpha|,\ \frac{-2}{K^+ + K^-}, 1\ )$$

The first three elements are $O(|\alpha|)$, corresponding to rows in $\mathbf{G}$ representing pure Dirichlet conditions. This is the second simplification observed in this example, that the vector $\mathbf{w^T}$ has relatively simple dependence on $|\alpha|$.

By simple calculation, we get:

$$\mathbf{w^T G}\ \tilde{\mathbf{U}}_{\mathbf{0n}} = 2\ |\alpha|\ \frac{(K^+ - K^-)q_1 + (K^+ + K^- + 2)q_2}{K^+ + K^-} \neq 0$$

to be the well-posedness criteria, that is

$$(K^+ - K^-)q_1 + (2 + K^+ + K^-)q_2 \neq 0. \tag{17}$$

The simplifications noted above are what lead to this particularly clear form. We note that in the physical situation described in [3], $q_2 < 0$ (liquid moves toward the two phase zone) and $q_1 \approx 0$ so we expect the well-posedness term in (17) to be negative.

We consider now the choice of residual velocity (15) for this case. For instance, if $\mathbf{v} = \mathbf{e}_5$ (the physical velocity choice), we have:

$$\lambda = 2\ |\alpha|\ \frac{(K^+ - K^-)q_1 + (K^+ + K^- + 2)q_2}{K^+ + K^-}.$$

This is a stable choice for velocity, considering the predicted sign of the term (17) above. However, when we consider $\alpha \to \infty$ (finer discretizations), we get a very stiff problem and the time step we take should be correspondingly small. Therefore, better numerical properties are obtained when we choose $\mathbf{v}$ such that λ is independent of wave number. This goal can be achieved by choosing residuals of Dirichlet conditions. In this case, we can choose $\mathbf{v}^T = \mathbf{e}_1$ (corresponding to the saturation condition), then

$$\lambda = 2\ \frac{(K^+ - K^-)q_1 + (K^+ + K^- + 2)q_2}{K^+ + K^- + 2}$$

and we have an optimal velocity to evolve the interface. Numerical validation of the superior performance of this residual velocity over the physical one is given in Section 5 below.

A straight forward calculation shows that for all problems of class $\tilde{C}$ identified at the end of section 2 similar results are obtained. That is, the vector $\mathbf{w}$ in (14) and (15) has terms of order α in entries corresponding to pure Dirichlet conditions and constant in entries corresponding to pure Neumann conditions. Also, only the two global fluxes corresponding to derivative quantities enter these expressions. Similar simplifications are found in other cases when the interface conditions separate into pure Dirichlet and pure Neumann conditions.

4.3 Extension to the 3-dimensional problem

The linear analysis is similar except that we assume an initial flat interface to be $z = 0$, and a small perturbation of driving function is given:

$$\mathbf{G}\tilde{\mathbf{U}} = \mathbf{b} + \epsilon \mathbf{f} e^{i\alpha x} e^{i\beta y} \tag{18}$$

then consequently we have updated solution and interface:

$$\eta \sim \eta_0 + \epsilon\eta_1 + \cdots$$

$$\mathbf{u} \sim \mathbf{u}_0 + \epsilon\mathbf{u}_1 + \cdots$$

where

$$\eta_1(x, y) = \hat{\eta}_1 e^{i\alpha x} e^{i\beta y}$$

Then the separable solutions of Laplacian equation $\Delta\mathbf{u} = 0$ are in form of:

$$\mathbf{u} = e^{i\alpha x} e^{i\beta y} \hat{\mathbf{u}}$$

where

$$\hat{\mathbf{u}} = \mathbf{c} e^{\mp\sqrt{\alpha^2+\beta^2}\, z}$$

and $\mathbf{c} = (A^+,\ A^-,\ B^+,\ B^-)^T$ is any arbitrary constant vector determined by the fixed boundary conditions. So we have:

$$\mathbf{u}_1 = \mathbf{c} e^{\mp\sqrt{\alpha^2+\beta^2}\, z} e^{i\alpha x} e^{i\beta y} \tag{19}$$

If we expand the solution along the new interface, we have:

$$\mathbf{u}(x, y, \eta(x, y)) = \mathbf{u}_0(x, y, 0) + \epsilon\eta_1 \mathbf{u}_{0z}(x, y, 0) + \epsilon\mathbf{u}_1(x, y, 0) + O(\epsilon^2) \tag{20}$$

and since the leading order term of interface is $\eta_0 = 0$, we can consider roughly $\mathbf{u_n} = \mathbf{u}_z$.

$$\mathbf{u_n}(x, y, \eta(x)) = \mathbf{u}_{0z}(x, y, 0) + \epsilon[\mathbf{u}_{1z}(x, y, 0) + \eta_1 \mathbf{u}_{0zz}(x, y, 0)] + O(\epsilon^2) \tag{21}$$

Substitute those expansions into (20), equating coefficients of different orders, we have:

$$[\mathbf{G}\tilde{\mathbf{U}}_1 + \hat{\eta}_1 e^{i\alpha x} e^{i\beta y} \tilde{\mathbf{U}}_{0\mathbf{n}}] = \mathbf{f}\, e^{i\alpha x} e^{i\beta y} \tag{22}$$

where $\tilde{\mathbf{U}}_{0\mathbf{n}} = (\mathbf{u}_{0zz}^T, \mathbf{u}_{0z}^T)^T$ is dependent on $\mathbf{u}_0$, and $\tilde{\mathbf{U}}_1 = (\mathbf{u}_{1z}^T, \mathbf{u}_1^T)^T$ with $\mathbf{u}_1$ in (3.15).

The base solution $\mathbf{u}_0$ in 3-D retains the same form in the 2-D case. We need the solutions independent of coordinate variables x and y, which lead to $\mathbf{u}_0 = z\mathbf{r}^1 + \mathbf{r}^0$, and consequently

$$(\mathbf{r}^1,\ \mathbf{r}^0)^T \in \mathcal{N}(\mathbf{G})$$

we always have $\tilde{\mathbf{U}}_{0\mathbf{n}} = (0, \mathbf{r}_1)^T$. Hence:

$$\tilde{\mathbf{U}}_{0\mathbf{n}} \in \mathcal{S}[\mathcal{N}(\mathbf{G})] = (\ \mathbf{0}_{3\times 4},\ \ \mathcal{N}(\mathbf{G})_{l4}\ )^T \tag{23}$$

where $\mathcal{N}(\mathbf{G})_{l4}$ represents the left four columns of $\mathcal{N}(\mathbf{G})$.

After we figure out $\tilde{\mathbf{U}}_{0\mathbf{n}}$, the next step is to find $\tilde{\mathbf{U}}_1$. We reserve the notation of matrix $\mathbf{M}$ to provide us a more clear structure of $\tilde{\mathbf{U}}_1$.

$$\tilde{\mathbf{U}}_1(x, y, 0) = (\mathbf{u}_{1z}, \mathbf{u}_1) = e^{i\alpha x} e^{i\beta y} \mathbf{M}\mathbf{c}$$

and

$$\mathbf{M} = \begin{pmatrix} \mp\sqrt{\alpha^2 + \beta^2} I_4 \\ I_4 \end{pmatrix}$$

where I_4 is a 4×4 identity matrix. Thus the equation (3.18) becomes

$$\mathbf{G}\mathbf{M}\mathbf{c} + \hat{\eta}_1 \mathbf{G}\tilde{\mathbf{U}}_{0\mathbf{n}} = \mathbf{f} \tag{24}$$

Denoting its left nullspace by $\mathbf{w} = \mathcal{N}[(\mathbf{G}\mathbf{M})^T]$, we still have the same criteria for well-posedness:

$$\mathbf{w}^{\mathbf{T}} \mathbf{G} \tilde{\mathbf{U}}_{0\mathbf{n}} \neq 0 \tag{25}$$

Applying this to our physical example in 3-D, we have:

$$\mathbf{w}^{\mathbf{T}} \mathbf{G}\ \tilde{\mathbf{U}}_{0\mathbf{n}} = 2\ \sqrt{\alpha^2 + \beta^2}\ \frac{(K^+ - K^-)q_1 + (K^+ + K^- + 2)q_2}{K^+ + K^-} \neq 0$$

This provides the same information as the 2-D problem. A study of the properties of interface velocities also gives results analogous to the 2-D case.

5 A 2-D computational example

In this section, we show how the residual velocities work on the vector Laplacian problem by computing the linear example of section 3. In addition to the interface conditions, the following fixed boundary

conditions are given: On the bottom, we assume the medium is saturated with liquid water, thus $s = 1$, and give a constant reference temperature

$$T^-(x, 0) = T_0.$$

On the top boundary, we make the boundary impenetrable to vapour

$$\frac{\partial P}{\partial \mathbf{n}} = 0$$

and take the heat flux to be given:

$$K^+ \frac{\partial T^+}{\partial \mathbf{n}} = f_1(x).$$

We take $f_1(x) = 2 + \sin(x)/2$ and $T_0 = 10$ as our numerical example. These conditions lead to a global flux $q_2 < 0$ (water flux upwards towards the interface) at each interface location. In the computations below, we take $K^+ = K_-$ so the well-posedness condition (17) is satisfied with the sign that makes our velocity sign choices stable.

5.1 Exact solution

In order to get an exact solution that can be compared with the numerical approximation, we start by building two piecewise functions

$$U = \begin{cases} K^+T^+ & \text{in } D^+ \\ K^-T^- - s & \text{in } D^- \end{cases} \qquad V = \begin{cases} P & \text{in } D^+ \\ T^- + s & \text{in } D^- \end{cases}$$

The two Laplacian equations $\Delta U = 0$ and $\Delta V = 0$ hold in the whole domain discarding the interface. The continuity gives the Neumann conditions across the interface:

$$K^+T^+_{\mathbf{n}} - K^-T^-_{\mathbf{n}} = -s_{\mathbf{n}} \qquad \text{and} \quad P_{\mathbf{n}} = T^-_{\mathbf{n}} + s_{\mathbf{n}}$$

and because $s = 0$ at the interface, the Dirichlet conditions across the interface are:

$$K^+T^+ = K^-T^- \qquad \text{and} \quad P = T^-$$

Note that only when $K^+ = K^-$, the problem is equivalent to our original one, so we set $K^+ = K^-$ and try to find the location of the interface $s = 0$. Solving the problem, we have:

$$T^+ = 9 + 2y + \frac{\sin(x)}{2}\frac{\sinh(y)}{\cosh(L)} \qquad P = 11$$

$$T^- = 10 + y + \frac{\sin(x)}{4}\frac{\sinh(y)}{\cosh(L)} \qquad s = 1 - y - \frac{\sin(x)}{4}\frac{\sinh(y)}{\cosh(L)}$$

and the location of $s = 0$ is given implicitly by

$$4(1-y)\cosh(L) - \sin(x)\sinh(y) = 0$$

By setting x equally distributed in the interval $[0, 2\pi]$, we can solve this transcendental equation for y, and thus find the coordinates of points on the interface to arbitrarily high precision.

5.2 Finite difference method in mapped rectangular domain

To handle the two irregular subdomains separated by curved interface, we map them into two rectangular domains, so that finite difference method can be naturally employed. A finite element method would be a good alternative for more irregular domains. A preliminary finite element implementation was done in [7] which required considerable grid refinement near the interface. The finite difference implementation given here demonstrates that this is not necessary for accurate solutions.

Suppose $y = h(x)$ is the known interface, we will do the following mapping:

$$\begin{aligned} D^+ : &\quad (x,y) \ \rightarrow (x_1 = x, \ \ y_1 = 1 + (y - h(x))/(L - h(x))) \\ D^- : &\quad (x,y) \ \rightarrow (x_2 = x, \ \ y_2 = y/h(x)) \end{aligned}$$

The new domain is $[0, 2\pi] \times [0, 2]$, and the interface $y = h(x)$ has been mapped into $y_1 = y_2 = 1$. Then by simple calculation, we have:

$$\begin{aligned} \frac{\partial T}{\partial x} &= \frac{\partial T}{\partial x_2}\frac{\partial x_2}{\partial x} + \frac{\partial T}{\partial y_2}\frac{\partial y_2}{\partial x} = \frac{\partial T}{\partial x_2} - \frac{h'(x_2)y_2}{h(x_2)}\frac{\partial T}{\partial y_2} \\ \frac{\partial T}{\partial y} &= \frac{\partial T}{\partial x_2}\frac{\partial x_2}{\partial y} + \frac{\partial T}{\partial y_2}\frac{\partial y_2}{\partial y} = \frac{1}{h(x_2)}\frac{\partial T}{\partial y_2} \end{aligned}$$

Note that $\frac{\partial x_2}{\partial y} = 0, \frac{\partial y_2}{\partial x} \neq 0$. Rewrite the Laplacian equations in the

mapped lower subdomain:

$$\begin{aligned}\Delta T^- &= \frac{\partial^2 T}{\partial y^2} + \frac{\partial^2 T}{\partial x^2} = \frac{1}{h(x_2)^2}\frac{\partial^2 T}{\partial y_2^2} + \frac{\partial x_2}{\partial x}\frac{\partial}{\partial x_2}\left(\frac{\partial T}{\partial x}\right) - \frac{h'(x_2)y_2}{h(x_2)}\frac{\partial y_2}{\partial x}\frac{\partial}{\partial y_2}\left(\frac{\partial T}{\partial x}\right) \\ &= \frac{1}{h(x_2)^2}\frac{\partial^2 T}{\partial y_2^2} + \frac{\partial x_2}{\partial x}\frac{\partial}{\partial x_2}\left(\frac{\partial T}{\partial x_2} - \frac{h'(x_2)y_2}{h(x_2)}\frac{\partial T}{\partial y_2}\right) \\ &- \frac{h'(x_2)y_2}{h(x_2)}\frac{\partial y_2}{\partial x}\frac{\partial}{\partial y_2}\left(\frac{\partial T}{\partial x_2} - \frac{h'(x_2)y_2}{h(x_2)}\frac{\partial T}{\partial y_2}\right) \\ &= \frac{1+h'(x_2)^2y_2^2}{h(x_2)^2}\frac{\partial^2 T^-}{\partial y_2^2} + \frac{\partial^2 T^-}{\partial x_2^2} - 2\frac{y_2 h'(x_2)}{h(x_2)}\frac{\partial^2 T^-}{\partial x_2 \partial y_2} \\ &+ \frac{2h'(x_2)^2 - h''(x_2)h(x_2)}{h(x_2)^2}y_2\frac{\partial T^-}{\partial y_2}\end{aligned} \tag{26}$$

Similar calculation gives the Laplacian equation in the mapped upper subdomain:

$$\begin{aligned}\Delta T^+ &= \frac{1+h'(x_1)^2(2-y_1)^2}{(L-h(x_1))^2}\frac{\partial^2 T^+}{\partial y_1^2} + \frac{\partial^2 T^+}{\partial x_1^2} - 2\frac{(2-y_1)h'(x_1)}{(L-h(x_1))}\frac{\partial^2 T^+}{\partial x_1 \partial y_1} \\ &- \frac{2h'(x_1)^2 + h''(x_1)(L-h(x_1))}{(L-h(x_1))^2}(2-y_1)\frac{\partial T^+}{\partial y_1}\end{aligned} \tag{27}$$

For the pressure P and saturation s, we get similar formulas. The Neumann interface and fixed boundary conditions should be reformulated as well in the new coordinates. For the Neumann (physical) velocity computation, we choose the residual of mass conservation condition $P_{\mathbf{n}} - T^-_{\mathbf{n}} - s_{\mathbf{n}} = 0$ to move the interface. Alternatively, the Dirichlet condition $s = 0$ is picked as the Dirichlet residual velocity.

In order to make our numerical approximation second order accurate, we use central difference scheme all through the discretization. With $N \times N$ to be the resolution on either side, the resultant coefficient matrix is of order $4N^2 \times 4N^2$.

5.3 The numerical results

We start from $N = 10$, and increase it to get higher accuracy. $L = 2$ is fixed all through the computation. To get the results in Table 1, we set the timestep $\Delta t = 0.02$ for the Neumann (physical) velocity, and compute till $T = 24$, which is long enough

Grids	errInf	ratio	errT	ratio	errS	ratio
10×10	0.0031	***	0.0075	***	2.8773e-5	***
20×20	8.0341e-4	3.859	0.0019	3.947	6.4194e-6	4.48
40×40	2.0019e-4	4.013	4.8504e-4	3.917	1.6205e-6	3.961

Table 1: Convergence test of Neumann residual velocity

Grids	errInf	ratio	errT	ratio	errS	ratio
10×10	0.0032	***	0.0075	***	2.9558e-5	***
20×20	8.0341e-4	3.983	0.0019	3.947	6.4127e-6	4.601
40×40	2.0019e-4	4.013	4.8504e-4	3.917	1.6201e-6	3.960

Table 2: Convergence test of Dirichlet residual velocity

to reach the steady state. The errors **errInf, errT, errS** are respectively the errors of interface, temperature and saturation in maximum norm. For the Dirichlet (artificial) residual velocity, we take $\Delta t = 0.2$, and iterate till $T = 24$, the errors are shown in Table 2. Note that at (almost) steady state, the errors of the two methods are (almost) identical since the discretization of the steady-state solution is identical.

Obviously, both methods have second order accuracy implied by the convergent rate. Now we try to demonstrate the advantage of the Dirichlet (artificial) residual velocity by setting the timestep Δt a free parameter. As we know, since we have to use explicit scheme for $\mathbf{x_n} = R(\mathbf{x})$ to evolve the interface, the timestep has to be reduced when refining the grid to make it within the stability region. In Table 3, we observe this property in Neumann residual velocity, but not in Dirichlet one. This means, even when we have very fine grids, the timestep can be kept reasonably large. Since we know in each time iteration, the computational complexity is almost the same, allowing larger timesteps can greatly reduce the computational cost.

In Table 3, **VN** and **VD** represent respectively the Neumann and Dirichlet residual velocities. It's not hard to see for Neumann residual velocity, $\Delta t = 0.12$ is appropriate for 10×10 grids to

Grids	timestep	RV	errInf	errT	errS
10×10	0.20	VN	0.9213	0.8734	0.1029
	0.15	VN	0.0453	0.0863	0.0122
	0.12	VN	0.0031	0.0075	2.8773e-5
10×10	0.20	VD	0.0032	0.0075	2.9558e-5
20×20	0.12	VN	12.0340	6.2583	0.8346
	0.08	VN	73.4589	4.9261	1.3080
	0.06	VN	8.0341e-4	0.0019	6.4194e-6
20×20	0.20	VD	8.0341e-4	0.0019	6.4127e-6
40×40	0.06	VN	9.6403	24.4088	0.9594
	0.04	VN	3.8939	3.5538	0.8762
	0.03	VN	2.0019e-4	4.8504e-4	1.6205e-6
40×40	0.20	VD	2.0019e-4	4.8504e-4	1.6201e-6

Table 3: Performance of different residual velocities

get convergence, and when we refine to 20×20, $\Delta t = 0.06$ is correspondingly decreased, and for 40×40, it becomes $\Delta t = 0.03$. However, we can use $\Delta t = 0.2$ for all three resolutions if the Dirichlet residual velocity is chosen. Considering the appropriate timesteps $\Delta t = 0.03$ and $\Delta t = 0.2$ when the resolution is 40×40, Dirichlet residual velocity is obviously better than the physical Neumann one.

6 Conclusions and discussion

Local, linear well-posedness criteria were developed for a general class of "2+2" vector Laplacian problems. Much simplification can be obtained in certain cases of physical interest. This is demonstrated in a simplified model of two-phase flow with phase change in porous media. The theory also allows the investigation of the stability and numerical properties of residual velocities to compute the steady state. It was possible to identify a superior velocity choice for the physical example and other problems in its general class. The theory was verified computationally using a finite difference method with mapped coordinates. In general,

this approach offers a way to improve the performance of certain steady-state interface computations with very little effort. Ongoing work suggests that these ideas can be extended to interface problems involving more general second order elliptic systems, such as problems from viscous, incompressible fluid flow. Extension to higher order problems with biharmonic operators are also possible. Efficient implementation of the method in a finite element framework is still an open problem.

Acknowledgement

This work is supported by NSERC and MITACS. We also acknowledge the valuable suggestions from Lloyd Bridge and Roger Donaldson.

References

[1] N. Al-Rawahi and G. Tryggvason (2004) *Numerical simulation of dendritic solidification with convection: three-dimensional flow*, J. Comput. Phys. 194:677-696.

[2] H.W.Alt and L.A.Caffarelli (1981) *Existence and regularity for a minimum problem with free boundary*, Journal fur die Reine und Angewandte Mathematik 325:105-144.

[3] L.Bridge, R.Bradean, M.J.Ward and B.R.Wetton (2003) *The analysis of a two-phase zone with condensation in a porous medium*, Journal of Engineering Mathematics, 45:247-268.

[4] R. Caflisch, F. Gibou, R. Fedkiw and S. Osher (2003) *A level set approach for the numerical simulation of dendritic growth*, J. Sci. Comput. 19:183-199.

[5] T. Cheng, P. Minev, and K. Nandakumar (2004) *A projection scheme for incompressible multiphase flow using adaptive Eulerian grids*, Int. J. Numer. Meth. Fluids, 45: 1-19.

[6] J.Crank (1984) *Free and moving boundary problems*, Clarendon, Oxford.

[7] R.Donaldson and B.R.Wetton (2004) *Solving steady interface problem using residual velocities*, accepted in the IMA Journal of Applied Mathematics, preprint available at www.math.ubc.ca/∼wetton/.

[8] J.Glimm, J.W.Grove and Y. Zhang (2002) *Interface tracking for axisymmetric flows*, Journal of Scientific Computation, 24(1): 208-236

[9] J.Haslinger, T.Kozubeck, K.Kinisch and G.Peichl (2003) *Shape optimization and fictitious domain approach for solving free boundary problems of bernoulli type*, Computational Optimization and Applications, 26:231-251.

[10] Z.Li (1997) *Immersed interface method for moving interface problems*, Numerical Algorithms 14:269-293

[11] S.Osher and J.A.Sethian (1988) *Fronts propagating with curvature-dependent speed: Algorithms based on Hamilton-Jacobian formulations*, Journal of Computational Physics, 100:209-228

[12] F.Raymond and J.M. Rosant (2000) *A numerical and experimental study of the terminal velocity and shape of bubbles in viscous liquids*, Chem. Eng. Sci. 55:943-955.

[13] J.Sokolowski and J.P.Zelesio (1992) *Introduction to shape optimization, shape sensitivity analysis*, Springer-Verlag, New York.

[14] M. Sussman, P. Smereka and S. Osher (1994) *A level set approach for computing solutions to incompressible 2-phase flow*, J. Comput. Phys. 114:146-159.

[15] T. Tiihonen (1997) *Shape optimization and trial methods for free boundary problems*, RAIRO, Math. Model. Numer. Anal. 31:805-825.

[16] S.O.Unverdi and G.Tryggvason (1992) *A front tracking method for viscous incompressible, multi-fluid flows*, Journal of Computatioanal Physics, 100:25-37

[17] Y.C.Tai, S.Noelle, J.M.N.T.Gray, and K.Hutter (2002) *Shock-Capturing and front tracking methods for Granular Avalanches*, Journal of Computational Physics 175,269-301

[18] D.E.Womble (1989) *A front-tracking method for multiphase free boundary problems*, Journal on Numerical Analysis, 26(2):380-396